ENVIRONMENTAL RESEARCH
LETTERS

LETTER • OPEN ACCESS

Rapid high-latitude cooling in the southeastern Pacific sector driven by North Atlantic warming during 1979–2013 in CESM1

To cite this article: Shuai-Lei Yao *et al* 2024 *Environ. Res. Lett.* **19** 064025

IOP Publishing Environ. Res. Lett. 19 (2024) 064025 https://doi.org/10.1088/1748-9326/ad4b45

ENVIRONMENTAL RESEARCH
LETTERS

OPEN ACCESS

RECEIVED
25 February 2024

REVISED
15 April 2024

ACCEPTED FOR PUBLICATION
14 May 2024

PUBLISHED
24 May 2024

LETTER

Rapid high-latitude cooling in the southeastern Pacific sector driven by North Atlantic warming during 1979–2013 in CESM1

Shuai-Lei Yao[1], **Renguang Wu**[2,*], **Pengfei Wang**[1,3] **and Shangfeng Chen**[3,4]

[1] State Key Laboratory of Numerical Modeling for Atmospheric Sciences and Geophysical Fluid Dynamics, Institute of Atmospheric Physics, Chinese Academy of Sciences, Beijing 100029, People's Republic of China
[2] School of Earth Sciences, Zhejiang University, Hangzhou 310058, People's Republic of China
[3] Center for Monsoon System Research, Institute of Atmospheric Physics, Chinese Academy of Sciences, Beijing 100029, People's Republic of China
[4] College of Earth and Planetary Sciences, University of Chinese Academy of Sciences, Beijing 100049, People's Republic of China
[*] Author to whom any correspondence should be addressed.

E-mail: renguang@zju.edu.cn

Keywords: rapid southeastern Pacific cooling, Rossby wave, tropical-Southern Ocean teleconnections, shortwave-low-cloud-SST feedback

Supplementary material for this article is available online

Abstract

During the 1979–2013 satellite observation period, the sea surface temperature (SST) has cooled substantially in the high-latitude Southern Ocean, with the most pronounced cooling tendency centered in the southeastern Pacific domain. Previous hypotheses have commonly ascribed the recent Southern Ocean cooling to either the tropical eastern Pacific cooling or North Atlantic and tropical Indian Ocean SST warming. However, the mechanisms underpinning significant cooling in the southeastern Pacific sector remain debatable. By diagnosing three pacemaker experiments with a state-of-the-art global climate model in which SSTs in the North Atlantic, tropical central-eastern Pacific, and tropical Indian Ocean-western Pacific are individually nudged to mimic the observed trajectory, we show that the North Atlantic dominates in the cold SST response of the southeastern Pacific sector during 1979–2013. Anomalous North Atlantic warming initiates a quasi-stationary Rossby wave response to a south-to-north cross-equatorial Hadley circulation strengthening, leading to an enhanced Amundsen Sea Low. As a result, due primarily to the increased low-level marine cloud cover, the net surface shortwave radiation reduction triggers rapid SST cooling in the southeastern Pacific domain. The southeastern Pacific cold SST anomalies are further maintained via the shortwave radiation-low-cloud-SST positive feedback on decadal timescales. Our results suggest that the shortwave radiation-low-cloud SST feedback is fundamental to the observed long-term cooling of the high-latitude Southern Ocean, with profound climate consequences worldwide.

1. Introduction

Despite continuous increase in the heat-trapping atmospheric greenhouse gas concentration during the satellite-monitoring period of 1979–2013, the observed sea surface temperature (SST) has experienced a cold-phase Inter-decadal Pacific Oscillation (IPO)-like anomaly in the whole Pacific basin (Power *et al* 1999) and conspicuous cooling in the high-latitude Southern Ocean (50° S–70° S; the blue box in figure 1), with prominent cold tendency occupying the southeastern Pacific domain (50° S–70° S and 160° W–80° W; the green box in figures 1(a) and (c)). The marked SST cooling across the tropical eastern Pacific and high-latitude Southern Ocean, prevalent in different observations (figure S1), generates anomalously negative climate feedback and partly counteracts the greenhouse gas-induced warming, thus contributing to the early twenty-first-century global warming slowdown (Meehl *et al* 2011, 2016, Kosaka and Xie 2013, Yao *et al* 2017) and accelerated Arctic sea-ice loss (Baxter *et al* 2019). However, the tropical Pacific and Southern Ocean SST-driven cooling effects, especially for recent decades (Stevens *et al*

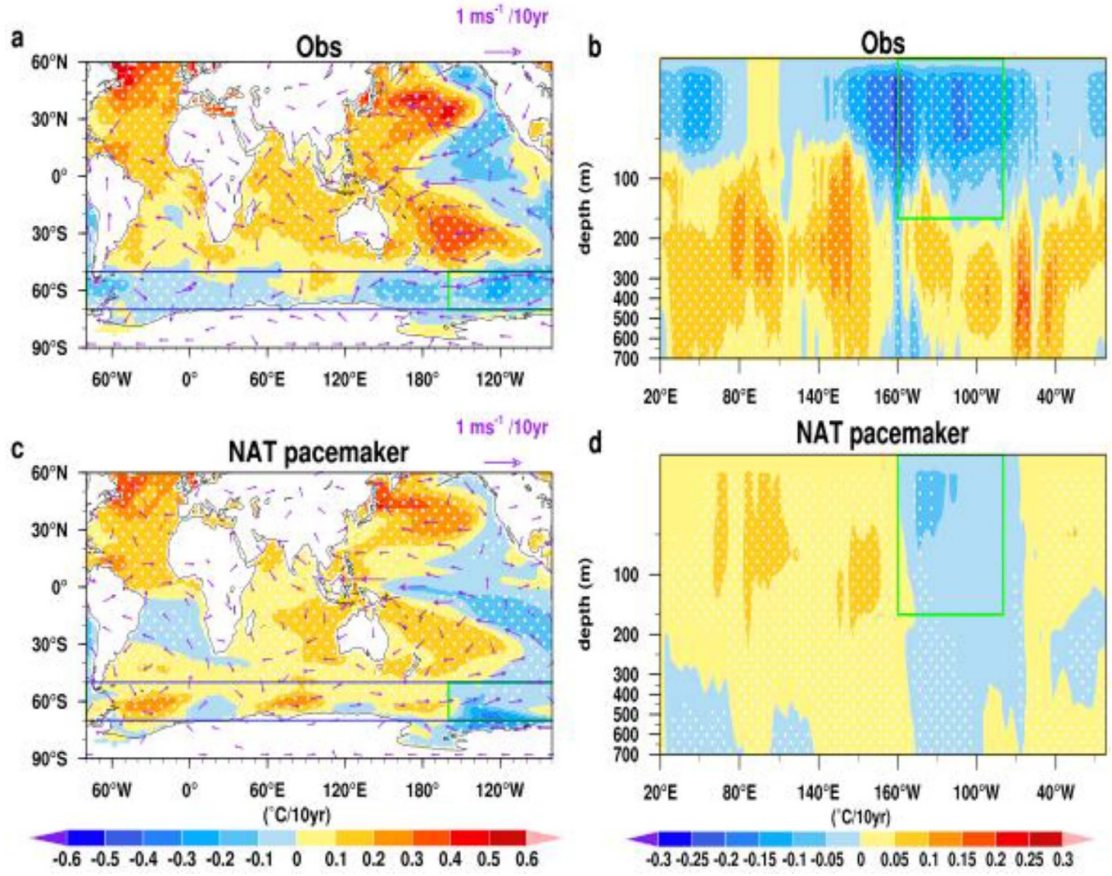

Figure 1. Linear trends of sea surface temperature (SST), 850 hPa winds, and meridional-mean sea water potential temperature (averaged over the zonal belt of 50° S–70° S) for observations (Obs); (a), (b) and North Atlantic Ocean pacemaker experiments (NAT); (c), (d) for 1979–2013. Observed trends are computed from ERSST v3b and an ensemble mean of four different reanalysis datasets, including 20CR3, ERA-interim, ERA5, JRA55 (a), and ORAS5 datasets (b). Simulated trends are estimated from the 10-member ensemble mean of North Atlantic Ocean pacemaker simulations (NAT); (c), (d). The green boxes in the left (a), (c) and right (b), (d) panels indicate surface and subsurface cold anomalies in the southeastern Pacific sector (50° S–70° S and 160° W–80° W outlined by the green box) of the high-latitude Southern Ocean (50° S–70° S demarcated by the blue box). Stipplings and vectors are only shown where trends are statistically significant above the 95% confidence level based on the Mann–Kendall test.

2016, Kang *et al* 2023), are misrepresented in almost all the global climate models participating in the sixth Coupled Model Inter-comparison Project (figure S2), rendering our low confidence in near-term climate predictions and future climate projections. Thus, uncovering the causes of significant cooling over the tropical Pacific and high-latitude Southern Ocean is pressing to provide accurate estimates of future global warming rates and determine the time of emergence of the 1.5 °C warming target.

Although the tropical Pacific cooling has been well recognized to be partly tied to the cold-phase IPO and partially forced by the North Atlantic warming related to the warm-polarity Atlantic Multidecadal Variability via the intensified Pacific Walker circulation (McGregor *et al* 2014, Li *et al* 2016, Ruprich-Robert *et al* 2017, Meehl *et al* 2021, Yao *et al* 2021, 2023), the mechanisms behind remarkable high-latitude Southern Ocean cooling remain controversial. One major hypothesis considers a strengthening of the poleward-shifted surface westerlies due to stratospheric ozone depletion (Sigmond and Fyfe 2010, Bitz and Polvani 2012, Ferreira *et al* 2015) and greenhouse gas increase (Hall and Visbeck 2002, Arblaster and Meehl 2006). The accelerated surface westerlies enhance northward Ekman advection of cold waters and cool the Southern Ocean (Hall and Visbeck 2002). Additionally, the enhanced surface freshening due to Antarctic ice-sheet and ice-shelf meltwater and sea-ice transport under greenhouse warming favors the increased stratification of vertical density and the suppressed mixing with warmer deep-layer waters, leading to the Southern Ocean cooling (Haumann *et al* 2016, 2020, Pauling *et al* 2016, Purich *et al* 2018). Alternatively, recent high-latitude Southern Ocean cooling may be caused by the ceased Weddell Sea deep convection of the Southern Ocean centennial-scale natural variability (Latif *et al* 2013, De Lavergne *et al* 2014, Zhang *et al* 2019). Because these above hypotheses are poorly represented in global climate models (Bourassa *et al* 2013, Haumann *et al* 2020), the timing, magnitude, and spatial pattern of high-latitude Southern Ocean cooling, particularly the southeastern Pacific, has yet to be rigorously quantified.

Besides those aforementioned local drivers, remote drivers originating from tropical SST variability are also invoked to explain the high-latitude Southern Ocean cooling. For example, not only tropical eastern Pacific cooling (Li *et al* 2021, Ibebuchi and Richman 2024) but also Atlantic or Indian Ocean warming (Li *et al* 2014, Simpkins *et al* 2014, 2016, Nuncio and Yuan 2015, Yuan *et al* 2018) can excite the Rossby wave trains that propagate poleward and ultimately induce the Southern Ocean SST changes. To what degree SST variability in individual basins creates significant cooling in the southeastern Pacific sector (50° S–70° S and 160° W–80° W; the green box in figures 1(a) and (c)) remains elusive. Our modeling study aims to gain deeper insight into the pronounced cooling in the southeastern Pacific sector. We first single out the main driver of rapid southeastern Pacific cooling in the high-latitude Southern Ocean. Then, we shed light on the dynamic pathways and physical process for the trans-hemispheric teleconnections.

2. Observations and model experiments

2.1. Reanalysis datasets

We utilize six different SST datasets to examine the robustness in the southeastern Pacific cooling during 1979–2013, including the NOAA Extended Reconstruction Sea Surface Temperature (ERSST) version 3b, 4, and 5 (Huang *et al* 2015, 2017), Centennial in situ Observation-Based Estimates SST (COBE-SST and v2) (Hirahara *et al* 2014), and Hurrell SST (Hurrell *et al* 2008). The observed southeastern Pacific cooling is not so sensitive to the choice of the ending year, such as 2013 and 2019 (figure S1). Due to the limited data coverage over the Southern Ocean before the 1970s (Smith *et al* 2008), we select the period 1979–2013 to better contrast with CMIP6 historical simulations in which the reliable time-varying radiative forcing ends in 2014. We also take four atmospheric reanalysis datasets to reveal the poleward-shifting westerly strengthening, including the NOAA twentieth-century reanalysis version 3 (20CR v3) (Slivinski *et al* 2019), the European Center for Medium-Range Weather Forecasts (ECMWF) Reanalysis (ERA-interim) and (ERA5) (Dee *et al* 2011), and the Japanese Reanalysis (JRA-55) (Kobayashi *et al* 2015) covering 1979–2013. The ECMWF oceanic reanalysis system (ORAS5) is used to inspect subsurface cold conditions of seawater potential temperature for 1979–2013. The reanalysis datasets above are summarized in table S1.

2.2. Pacemaker experiments

To delve into the potential drivers of significant southeastern Pacific cooling, we evaluate three time-evolving pacemaker experiments with the Community Earth System Model version 1.1 (CESM1) following the methodology of previous studies (Kosaka and Xie 2013, Deser *et al* 2017, Meehl *et al* 2021). The good performance of CESM1 in capturing tropical Pacific and Atlantic climate variability has been identified in earlier studies (e.g. Deser *et al* 2017, Meehl *et al* 2021). In these simulations (table S2), SST anomalies in the North Atlantic (NAT: 5° – 55° N, the American coast to Africa/Europe with 5° tapering buffer zones in southern and northern boundaries), tropical central-eastern Pacific (TEP: 15° S–15° N, 180° to the American coast with 5° buffer zones in the western, northern, and southern boundaries), and tropical Indian Ocean-western Pacific (IOWP: 15° S–15° N, African coast to 174° E with 5° buffer zones in the eastern, northern, and southern boundaries) are separately nudged to the observed trajectories (figure S3). Outside the nudging regions, the ocean-air systems are free to evolve and fully coupled. Each run is also forced with historical radiative forcing (1920–2005) and RCP8.5 scenario (2006–2013). It consists of ten ensemble members initialized with slightly different initial atmospheric conditions. The pacemaker experimental setup enables us to systematically investigate the extent to which SST variability in each basin produces climate changes in the high-latitude Southern Ocean.

All the linear trends from observations and pacemaker experiments presented here are estimated using Sen's slope method (Sen 1968), with a 95% statistical significance according to the Mann–Kendall test.

3. Results

3.1. Observed and simulated climate changes in the high-latitude Southern Ocean

We first examine the role of North Atlantic warming in driving climatic changes in the high-latitude Southern Ocean by constraining North Atlantic SST anomalies to observations in the pacemaker experiments. Figure 1 compares observed and simulated linear trends of SST, 850 hPa winds, and ocean potential temperature for 1979–2013. For observations, significant surface and subsurface cooling occur across a large swath of the Southern Ocean (south of 50° S), with the largest cooling signal concentrated in the southeastern Pacific and penetrating deep into ∼150 m (figures 1(a) and (b)), except for small patches of warming at the surface (50° S–70° S) and in the subsurface (90° E–110° E) of the Indian Ocean. Correspondingly, a strengthening of westerly winds in the Southern Ocean is also evident compared to the climatological mean westerlies north of 70° S (cf figures 1(a) and S4). In the southeastern

Pacific domain (50° S–70° S and 160° W–80° W), the SST cooling and westerly wind trends reach −0.117 °C/10 yr and 0.151 ms^{-1}/10 yr, respectively, similar to earlier findings of different data sources (Armour *et al* 2016, Jones *et al* 2016, Zhang *et al* 2019, 2021, Xu *et al* 2022). North Atlantic pacemaker simulations reproduce observed trends in the southeastern Pacific domain relatively well, with SST cooling of −0.074 °C/10 yr and westerly wind strengthening of 0.183 ms^{-1}/10 yr (figure 1(c)). Remarkably, the North Atlantic warming-induced surface and subsurface cooling signals are mainly limited to the southeastern Pacific sector (figures 1(c) and (d)), with comparatively weaker magnitudes than observations. The simulated subsurface cooling extends downward to a deeper depth (∼700 m), distinct from the observed surface cooling and subsurface warming (cf figures 1(d) and (b)). The observation-model mismatch may be due to the unrealistic representation of sea-ice-ocean freshwater fluxes by the lack of Antarctic glacial meltwater increase in global climate models (Bourassa *et al* 2013, Bronselaer *et al* 2020, Haumann *et al* 2020, Rye *et al* 2020). Surface cooling and the underestimated high-latitude freshwater flux induce the reduced density stratification and the deeper mixed layer (Gupta *et al* 2009), thus allowing surface cooling to intrude into a deeper layer with persistence.

To fully understand the remote drivers of rapid southeastern Pacific cooling, we quantify the respective contributions of the TEP cooling and IOWP warming using pacemaker experiments (figure S5). The TEP pacemaker simulations produce weak warming in the southeastern Pacific and significant warming in other parts of the high-latitude Southern Ocean (figure S5(a)). The IOWP pacemaker experiments also create extensive warming in the high-latitude Southern Ocean (figure S5(b)). Although both simulations replicate the intensified westerlies in the Southern Ocean, the southeastern Pacific warming response fundamentally disagrees with the observed and the North Atlantic warming-forced cooling (figure 1). Furthermore, previous studies report that stratospheric ozone loss possibly contributes to the Southern Ocean surface cooling through the poleward-intensifying westerlies associated with a positive-phase Southern Annular Mode (SAM) (Fyfe *et al* 2007, Ferreira *et al* 2015, Kostov *et al* 2017, Ibebuchi 2021). We systematically assess the importance of stratospheric ozone-depleting on the Southern Ocean SST changes by analyzing the stratospheric ozone single-forcing historical experiments of five CMIP6 models (figure S6). The southeastern Pacific SST response is ambiguous and varies widely across models. These model results demonstrate that North Atlantic warming contributes more to cooling in the southeastern Pacific sector for 1979–203.

3.2. Dynamics governing North Atlantic warming to force the southeastern Pacific cooling

Next, we unravel the dynamic pathways by which the North Atlantic SST warming signal is conveyed to the high-latitude Southern Ocean. North Atlantic pacemaker experiments well reproduce an enhanced north-minus-south meridional SST gradient across the tropical Atlantic (Levine *et al* 2018), albeit with larger cooling in the tropical South Atlantic than observations (cf figures 1(a) and (c)). In response to anomalous North Atlantic warming, a strong Atlantic inter-tropical convergence zone migrates northward and resides north of the equator (cf the increased precipitation trend and climatological-mean precipitation in figure 2(a)). The associated atmospheric convective heating induces anomalous tropospheric upper-level divergence extending from the equatorial Atlantic to the tropical North Atlantic and anomalous convergence over the South Atlantic (figure 2(b)). Consequently, these atmospheric perturbations result in a northward-extended strengthened Hadley circulation (figure 2(c)). While the North Atlantic warming-forced Hadley cell adjustment is initially local, the succeeding perturbation is large enough to affect the zonal-mean meridional stream functions (figure 2(c)). The descending branch of Hadley circulation intensification favors the increased upper-level convergence in the subtropical South Atlantic, ultimately forming anomalous Rossby wave sources south of the subtropical jet (Simpkins *et al* 2014, Li *et al* 2015, 2021).

The atmospheric circulation anomalies favor an equivalent barotropic Rossby wave pathway spreading from the mid-to-upper-level troposphere in the mid-to-high Southern Hemisphere (figures 2(d) and (e)). Specifically, a Rossby wave train initially emanates from the subtropical South Atlantic. Then, it propagates eastward within the climatological mean subtropical jet, ending over the Amundsen and Bellingshausen Seas following a great arc. This Rossby wave response features a distinctive zonal wavenumber-3 structure of alternating low-pressure and high-pressure anomalies of active centers (figures 2(d) and (e)), manifesting as a deepened Amundsen Sea Low and a positive-polarity SAM (Li *et al* 2014, Simpkins *et al* 2014). A dipole-like sea level pressure pattern, with anomalous high-pressure centers near 40° S and low-pressure centers near 65° S (Thompson and Wallace 2000, Ding *et al* 2012), characterizes a positive-phase SAM anomaly (figure 2(f)), corresponding to the poleward-shifted westerly wind intensification (figure 1(c)).

Indeed, the trans-hemispheric North Atlantic-Southern Ocean teleconnections are established via a two-pronged pathway: a direct Rossby wave response to a northward-displaced accelerated Hadley circulation induced by North Atlantic warming and an indirect response to a southward-shifted weakened

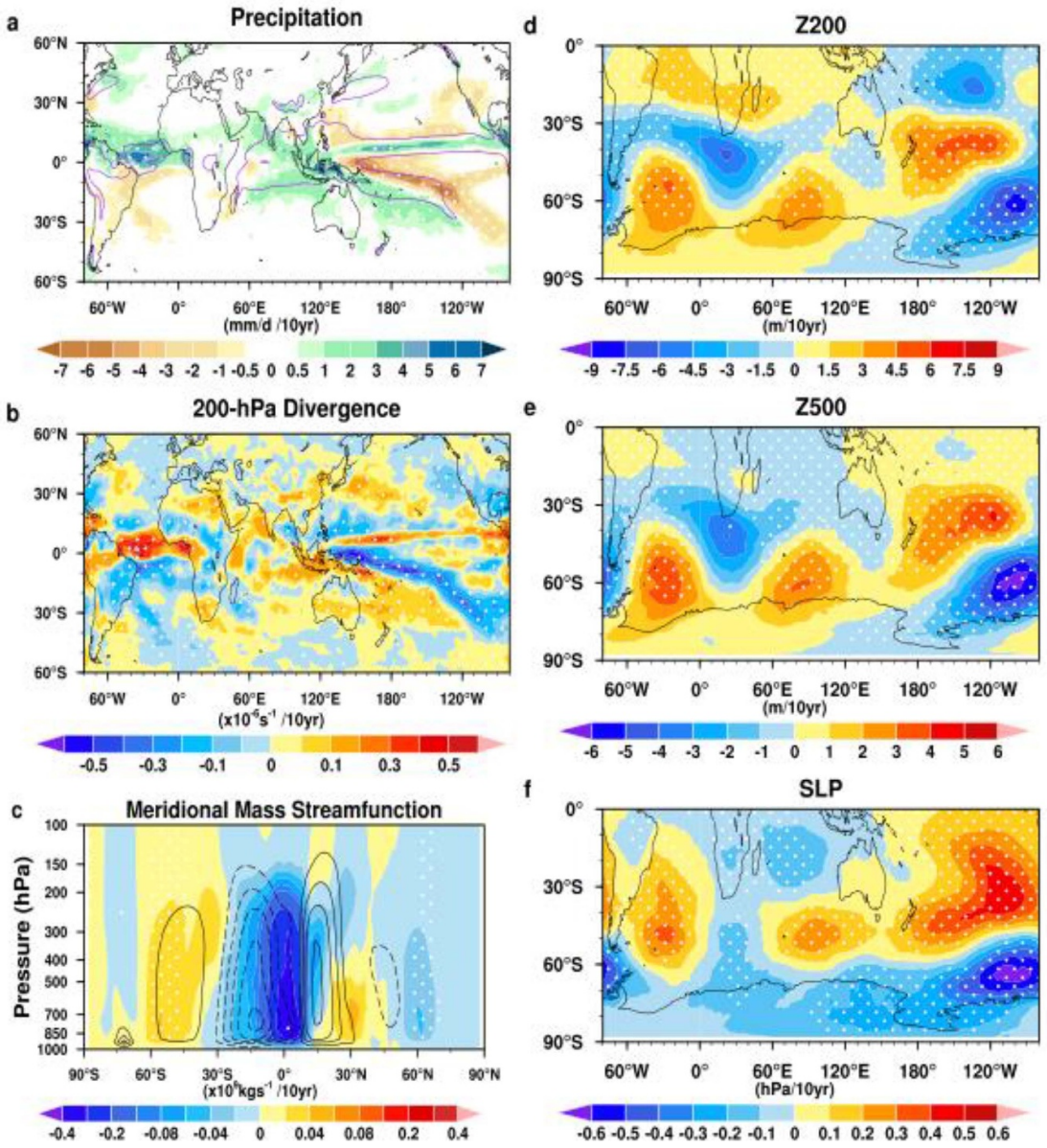

Figure 2. Dynamic pathway for North Atlantic warming to generate the Southern Hemisphere extratropical circulation changes. Linear trends of precipitation (a); units in mm d^{-1}, 200 hPa divergence (b); units in 10^{-6} s^{-1}, meridional mass stream function (c); 10^{10} kg s^{-1}, 200 hPa geopotential height (d); (Z200), 500 hPa geopotential height (e); (Z500), and sea level pressure (f); (SLP) for 1979–2013. The purple solid lines in (a) denote the climatological precipitation of 60 mm d^{-1}. The black lines represent the climatological meridional mass stream function (dashed contours for negative and solid contours for positive values) with an interval of 0.2×10^{11} kg s^{-1} from -1.0×10^{11} kg s^{-1} to 1.0×10^{11} kg s^{-1}. Positive values indicate the clockwise flow and vice versa. The zonal mean of Z200 (d) and Z500 (e) at each latitude has been removed to illustrate the propagation of the Rossby wave train. Results are computed from the 10-member ensemble mean of North Atlantic Ocean pacemaker simulations. Stippling signifies regions where trends are statistically significant above the 95% confidence level according to the Mann–Kendall test.

Hadley cell due to TEP cooling forced by North Atlantic warming (figures 2 and S7). In TEP pacemaker simulations (figure S7), meridionally wide tropical Pacific cooling tied to a cold-phase IPO and a strong southwestward-shifted South Pacific Convergence Zone (SPCZ) work together to produce the Rossby wave sources located south of the SPCZ (Folland *et al* 2002, Clem and Fogt 2015, Brown *et al* 2020). As such, a distinct Rossby wave pathway is formed, which is initially excited in the subtropical western South Pacific and then propagates eastward to traverse the Southern Ocean in a great circle (figure S7). This strong Rossby wave response translates well into a larger positive-polarity SAM anomaly and a stronger strengthening of the poleward-extended westerly winds (figure S5) than those induced by North Atlantic warming (figures 1(c) and 2(f)). While tropical Pacific cooling causes much stronger westerly winds in the southeastern Pacific, the marked southeastern Pacific cooling is more sensitive to North Atlantic warming than TEP cooling, suggesting that the key physical processes might be required to resolve the intriguing paradox.

3.3. Physical processes underlying the pronounced southeastern Pacific cooling response to North Atlantic warming

We further disentangle the primary physical processes responsible for North Atlantic warming to drive the significant cooling in the southeastern Pacific sector. Because the ocean mixed-layer heat balance governs the Southern Ocean SST changes (Dong *et al* 2007, Sallée *et al* 2010, Xu *et al* 2022), we determine the relative importance of thermodynamic components (surface heat flux in the first four terms below) and ocean dynamic components (Ekman and Geostrophic horizontal advection, diffusive process, and Entrainment process in the last four terms) based on the mixed-layer heat budget analysis as follows (Dong *et al* 2007):

$$\frac{\partial T}{\partial t} = \frac{1}{\rho_0 C_p h_m}\left(Q_{sw} + Q_{lw} + Q_{lh} + Q_{sh}\right) - \overrightarrow{V_E}\cdot\nabla T - \overrightarrow{V_G}\cdot\nabla T + \kappa_H \nabla^2 T + \frac{w_e\left(T_b - T\right)}{h_m} \quad (1)$$

where T, T_b, and h_m represent SST, sea water potential temperature below the mixed-layer depth, and the mixed-layer depth, respectively; ρ_0 (1027 kg m^{-3}) denotes the seawater reference density; C_p (4000 J kg^{-1} K^{-1}) signifies the seawater-specific heat capacity at constant pressure; Q_{sw}, Q_{lw}, Q_{lh}, and Q_{sh} are net surface shortwave radiation, longwave radiation, latent, and sensible heat flux, respectively; $\overrightarrow{V_E}$ and $\overrightarrow{V_G}$ indicate Ekman and Geostrophic current velocities, respectively; κ_H (500 m^2 s^{-1}) is the eddy diffusivity; w_e is the entrainment rate derived from the Ekman vertical velocity. We discard the downward shortwave radiative flux through vertical turbulent mixing and seawater absorption of the mixed layer due to its negligible effect relative to other terms in the equation (1).

We focus on the spatial distribution of individual term trends to better identify the principal physical factors controlling pronounced southeastern Pacific cooling (figure 3). Amongst all the surface heat fluxes, the net shortwave radiation reduction best matches the spatial pattern of southeastern Pacific SST cooling during 1979–2013 (cf figures 3(a) and 1(c)). Consistently, the area-averaged cooling trend caused by the diminished net shortwave radiation is −0.06 °C/10 yr, accounting for ∼81% of the southeastern Pacific SST cooling response to anomalous North Atlantic warming (−0.074 °C/10 yr in figure 1(c)). Although the reduced net surface longwave radiation, latent, and sensible heat fluxes contribute potentially to cooling in some parts of the southeastern Pacific domain (figures 3(b)–(d)), their spatial patterns are strikingly at odds with the distribution of marked southeastern Pacific cooling.

By comparison, ocean dynamic processes cannot properly explain remarkable cooling in the southeastern Pacific domain. Large warming north and small cooling south of 65° S caused by Ekman horizontal advection, especially the meridional Ekman transport, are seen over the southeastern Pacific (figure 3(e)). The north-south opposing responses of Ekman advection are mainly controlled by anomalous easterly-induced southward Ekman advection of warm waters and anomalous westerly-driven equatorward Ekman advection of cold waters (Hall and Visbeck 2002, Fyfe *et al* 2007, Bitz and Polvani 2012). The zonal distributions of Ekman advection and meridional Ekman transport also closely align with surface zonal wind stress (figure S8). Furthermore, the southeastern Pacific SST trends linked to the geostrophic advection are highly irregular, quite inconsistent with the spatial pattern of marked southeastern Pacific cooling response to North Atlantic warming (cf figures 3(f) and 1(c)), even though some cooling patches emerge. The effects from diffusion and entrainment processes are mostly negligible (figures 3(g) and (h)) and do not conform to the southeastern Pacific cooling pattern. The quantitative assessment provides evidence that the net surface shortwave radiation reduction is an important process underlying the significant southeastern Pacific cooling response to anomalous North Atlantic warming.

Previous observation-based and coupled model-based studies emphasize that the increasing westerly-driven northward Ekman advection of cold waters contributes to the Southern Ocean basin-scale cooling (Hall and Visbeck 2002, Dong *et al* 2007, Bitz and Polvani 2012, Kostov *et al* 2017, Xu *et al* 2022). Yet, North Atlantic pacemaker simulations fail to capture the large-scale cooling effects from the enhanced northward Ekman transport of cold waters (figure 3(e)). Although there is a broad agreement on the zonal-mean distributions of SST cooling and northward Ekman transport of cold waters south of 65° S across the southeastern Pacific sector (figure S8), the SST cooling responses to equatorward Ekman advection of colder waters are minimal. A possible explanation is that, in response to the poleward-shifted westerly wind intensification linked to a positive-polarity SAM anomaly, the initial fast cooling response lasts for a few years, and, after about ten years, it gradually begins to be overwhelmed by the accelerated upwelling of warmer deep-layer waters (Ferreira *et al* 2015, Kostov *et al* 2017) and additionally enhanced by the eddy compensation-induced warming (Doddridge *et al* 2019). This modeling evidence is compatible with the statistical analysis that the direct impact of the SAM on the southeastern Pacific sector is relatively weak over a long period (see text S1 in the supplementary information for more details). Thus, the net surface shortwave radiation reduction is more efficient in triggering and maintaining the SST cooling over the southeastern Pacific domain on decadal timescales (e.g. three decades or even longer).

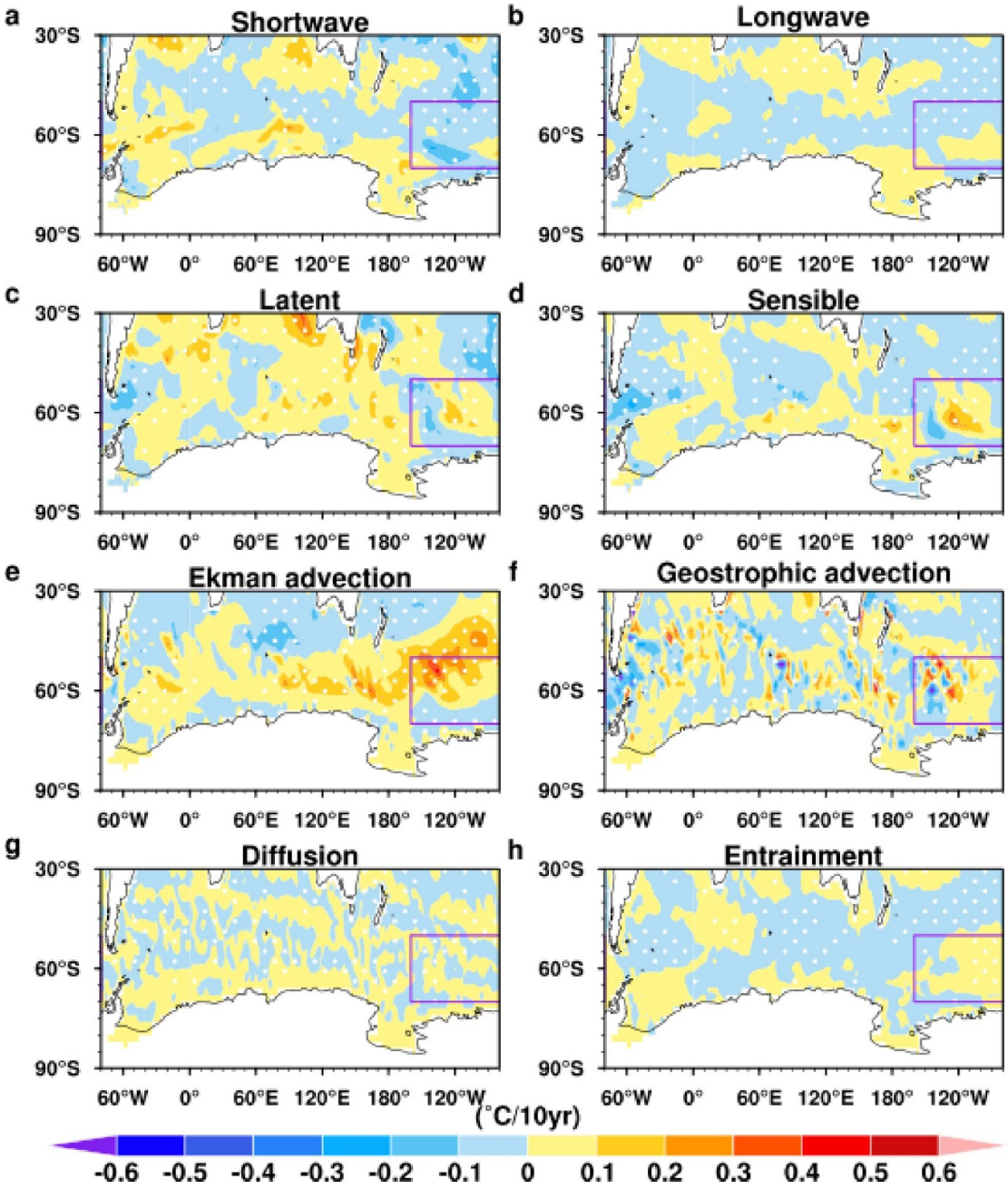

Figure 3. Physical processes for North Atlantic warming driving the Southern Ocean SST changes. The Southern Ocean SST changes are governed by net surface shortwave radiation (a), net surface longwave radiation (b), latent heat flux (c), sensible heat flux (d), horizontal Ekman advection (e), horizontal geostrophic advection (f), diffusion (g), and entrainment (h) during 1979–2013. Positive radiation flux downward denotes that the ocean absorbs heat from the atmosphere, thus heating the Southern Ocean SST. In contrast, negative radiation flux upward indicates that the ocean loses heat to the atmosphere, thus cooling the Southern Ocean. Negative (Positive) values in (e) denote the northward (southward) Ekman transport of cold (warm) waters, cooling (heating) the Southern Ocean SST. The purple box denotes the southeastern Pacific sector of the high-latitude Southern Ocean (50° S–70° S and 160° W–80° W). Results are calculated from the 10-member ensemble mean of North Atlantic Ocean pacemaker simulations. Stipplings denote regions where trends are statistically significant above the 95% confidence level based on the Mann–Kendall test.

We notice that the spatial pattern of net surface shortwave radiation mostly agrees with changes in the net shortwave radiation at the top of the atmosphere (figures 3(a) and 4(a)), particularly in the South Pacific (south of 30° S) in association with variations in cloud cover (figures 4(b) and (c)). The total cloud cover, mainly in the low-level troposphere, increases markedly in regions where the net shortwave radiation at the top of the atmosphere significantly declines. Eventually, the resulting net surface shortwave radiation reduction facilitates SST cooling trends in the South Pacific. The enhanced mid-level cloud cover may attenuate the net surface shortwave radiation in the southeastern Pacific sector and

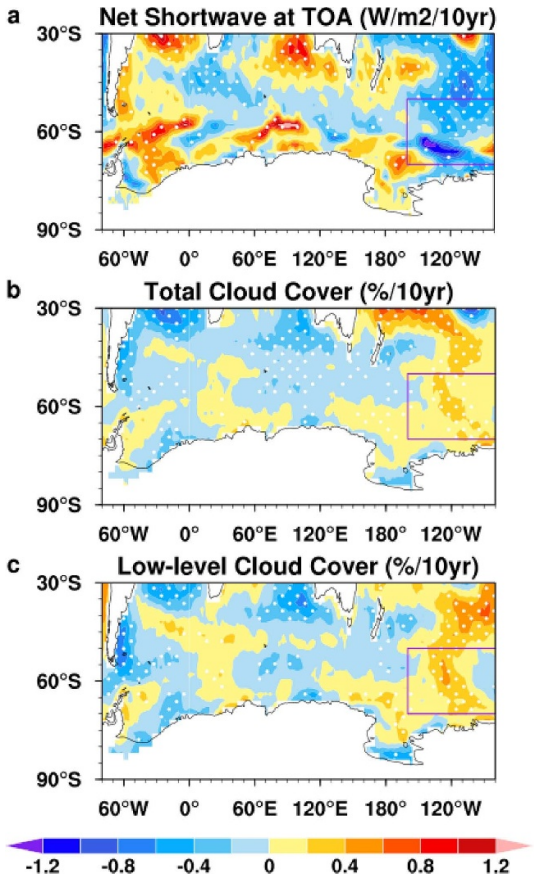

Figure 4. Responses of net shortwave radiation at the top of the atmosphere and cloud cover to the North Atlantic warming forcing. Linear trends of net shortwave radiation at the top of the atmosphere (a), total cloud cover (b), and low-level cloud cover (c) during 1979–2013. Positive (Negative) values for the net shortwave radiation flux at the top of the atmosphere go downward (upward). Positive (Negative) values for the cloud cover denote the cloud cover increases (reduction). Results are computed from the 10-member ensemble mean of North Atlantic Ocean pacemaker simulations. The purple box in each panel indicates the southeastern Pacific sector of the high-latitude Southern Ocean (50° S–70° S and 160° W–80° W). Stipplings domains are statistically significant above the 95% confidence level based on the Mann–Kendall test.

cool the SST there (figure S9). Still, it cannot reasonably explain the reduced net shortwave radiation at the surface and the top of the atmosphere in other parts of the South Pacific. As anomalous cold SSTs occur in the southeastern Pacific domain, the low-level marine cloud cover tends to increase, and more incident solar radiation is reflected into space, thus leading to further SST cooling and additional cloud formation (Mechoso *et al* 2014, 2016). Such favorable conditions are likely to trigger the shortwave radiation-low-cloud-SST positive feedback that helps to maintain the multidecadal SST cooling of the southeastern Pacific. These results suggest that the shortwave radiation-low-cloud-SST positive feedback dominates over the southeastern Pacific cold SST response to anomalous North Atlantic warming on decadal timescales. Notably, since the cloud cover is negligible and, subsequently, the shortwave radiation-low-cloud-SST positive feedback is minor, a slight warming appears in the southeastern Pacific sector in response to anomalous TEP cooling tied to a cold-phase IPO (see text S2 in the supplementary information for more details).

4. Summary and discussion

During 1979–2013, the observed Southern Ocean SST cooled considerably, with the largest and most consistent cooling trends in the southeastern Pacific sector among different observations (figure S1). Using three pacemaker experiments with CESM1 wherein SSTs in the North Atlantic, TEP, and tropical Indian-western Pacific are separately nudged to follow the observed evolutions, we systematically quantify the respective role of SST variability in each basin in generating SST changes in the southeastern Pacific domain. North Atlantic nudging simulations capture the observed significant cooling in the southeastern Pacific well, while the remaining two pacemaker experiments produce anomalous warming there. We further elucidate the dynamic process through which North Atlantic warming drives rapid southeastern Pacific cooling. Anomalous North Atlantic warming induces a northward-migrated enhanced Hadley circulation. Subsequently, it excites a quasi-stationary Rossby wave train traversing the high-latitude Southern Ocean, culminating with a deepened Amundsen Sea Low. As a result of the heightened low-level marine cloud cover, the net surface shortwave radiation reduction cools the southeastern Pacific. The southeastern Pacific cold SST response to anomalous North Atlantic warming is further maintained via the shortwave radiation-low-cloud-SST positive feedback on decadal timescales. Here, we highlight that the CESM1 pacemaker simulations are not intended to offer exact details of the marked southeastern Pacific cooling response during 1979–2013 but to systematically evaluate the respective role of individual ocean basins.

A new aspect of the study is that we employ the identical pacemaker experimental framework to rigorously quantify the relative importance of SST variability in three ocean basins, including the North Atlantic, TEP, and tropical IOWP, in forcing the high-latitude Southern Ocean SST changes. We argue that North Atlantic warming is decisive for driving the observed multidecadal SST cooling of the southeastern Pacific sector, whereas earlier studies have widely stressed the role of tropical Pacific and Indian Ocean SSTs (Simpkins *et al* 2016, Yuan *et al* 2018, Li *et al* 2021, Chung *et al* 2022). Distinct from the observed Southern Ocean broad cooling, North Atlantic pacemaker simulations capture only the southeastern Pacific cooling, implying that the observed cooling in other parts of the Southern Ocean is probably related to the Southern Ocean internal variability as

a consequence of the halted Weddell Sea deep convection (Latif *et al* 2013, Cabré *et al* 2017, Zhang *et al* 2019). Given that our analysis is solely building on the CESM1 (Deser *et al* 2017, Meehl *et al* 2021), the multi-model pacemaker experiments are urgently needed to reliably determine the relative importance of the North Atlantic SST variability and Southern Ocean internal variability in generating the observed long-term cooling of the Southern Ocean basin-scale SST.

Our results report that the shortwave radiation-low-cloud-SST positive feedback is key to the observed multidecadal cooling of the southeastern Pacific sector. However, the shortwave radiation-low cloud feedback is misrepresented in the current global climate models participating in the CMIP6 (Mechoso *et al* 2014, 2016, Zelinka *et al* 2020). For example, the equilibrium climate sensitivity in CMIP6 is higher on average than in previous generations of Coupled Model Inter-comparison Project, owing mostly to the stronger low cloud-SST positive feedback over the Southern Ocean through more dramatic reductions in low cloud amount and smaller increases in cloud liquid water (Zelinka *et al* 2020). These systematic biases greatly reduce the validity of the model attribution of Southern Ocean climatic changes to anthropogenic warming in recent decades. While early modeling studies of constraining tropospheric wind changes in global climate models attempt to uncover the causes of observed multidecadal Southern Ocean cooling (Pauling *et al* 2016, Blanchard-Wrigglesworth *et al* 2021), unraveling the large biases involving the absence of simulated Southern Ocean cooling, enhanced surface freshening, and Antarctic sea-ice modest increases remains challenging. Reducing these biases in global climate models through improving cloud physical processes and constraining the incoming shortwave radiation flux in the Southern Ocean might provide new insight into the origin of recent climate consequences in the Southern Ocean (Mechoso *et al* 2016), with far-reaching implications for the Antarctic sea-ice paradox (Li *et al* 2014).

Data availability statements

The reanalysis datasets used here are publicly available following the websites: the 20-century reanalysis product version 3 (https://psl.noaa.gov/data/gridded/index.html), ERA-interim (https://apps.ecmwf.int/datasets/data/interim-full-daily/levtype=sfc/), ERA5 (https://cds.climate.copernicus.eu/#!/search?text=ERA5&type=dataset), JRA55 (https://climatedataguide.ucar.edu/climatedata/jra55#:~:text=JRA%2D55%20is%20the%20first,%2DVar)%20to%20this%20period). ORAS5 datasets are available at https://cds.climate.copernicus.eu/cdsapp#!/search?type=dataset&text=ORAS5. All SST datasets used in this study are downloaded from the following websites: ERSST v3b, v4, and v5 (www.ncei.noaa.gov/products/extended-reconstructed-sst). COBE SST and COBE2 SST (https://psl.noaa.gov/data/gridded/index.html), Hurrell SST (https://psl.noaa.gov/data/gridded/). All model outputs are available at www.earthsystemgrid.org/dataset/ucar.cgd.ccsm4.output.html.

All data that support the findings of this study are included within the article (and any supplementary files).

Acknowledgments

This work is supported by the Strategic Priority Research Program of the Chinese Academy of Sciences (XDB0500303), the National Key R&D Program for Developing Basic Sciences (2020YFA0608902), and the National Science Foundation of China (NSFC42192563 and 42120104001). We are indebted to the high-performance computing support from Tianhe (www.nscc-tj.cn), sponsored by the National Supercomputer Center in Tianjin. We acknowledge the Community Earth System Model (CESM) large ensemble community project, climate variability, and change working group for making model output available. We also acknowledge the World Climate Research Programme working group on the coupled modeling, which led the design of CMIP6 experiments and coordinated the work. We are also grateful to the individual climate modeling group for their efforts in model simulations.

Conflict of interest

The authors declare no competing interests.

ORCID iDs

Renguang Wu https://orcid.org/0000-0003-4712-2251
Shangfeng Chen https://orcid.org/0000-0003-4347-8592

References

Arblaster J M and Meehl G A 2006 Contributions of external forcings to southern annular mode trends *J. Clim.* **19** 2896–905
Armour K C, Marshall J, Scott J R, Donohoe A and Newsom E R 2016 Southern Ocean warming delayed by circumpolar upwelling and equatorward transport *Nat. Geosci.* **9** 549–54
Baxter I *et al* 2019 How tropical Pacific surface cooling contributed to accelerated sea ice melt from 2007 to 2012 as ice is thinned by anthropogenic forcing *J. Clim.* **32** 8583–602
Bitz C and Polvani L M 2012 Antarctic climate response to stratospheric ozone depletion in a fine resolution ocean climate model *Geophys. Res. Lett.* **39** L20705
Blanchard-Wrigglesworth E, Roach L A, Donohoe A and Ding Q 2021 Impact of winds and Southern Ocean SSTs on Antarctic sea ice trends and variability *J. Clim.* **34** 949–65

Bourassa M A et al 2013 High-latitude ocean and sea ice surface fluxes: challenges for climate research Bull. Am. Meteorol. Soc. 94 403–23
Bronselaer B et al 2020 Importance of wind and meltwater for observed chemical and physical changes in the Southern Ocean Nat. Geosci. 13 35–42
Brown J R, Lengaigne M, Lintner B R, Widlansky M J, van der Wiel K, Dutheil C, Linsley B K, Matthews A J and Renwick J 2020 South Pacific convergence zone dynamics, variability and impacts in a changing climate Nat. Rev. Earth Environ. 1 530–43
Cabré A, Marinov I and Gnanadesikan A 2017 Global atmospheric teleconnections and multidecadal climate oscillations driven by Southern Ocean convection J. Clim. 30 8107–26
Chung E-S, Kim S-J, Timmermann A, Ha K-J, Lee S-K, Stuecker M F, Rodgers K B, Lee S-S and Huang L 2022 Antarctic sea-ice expansion and Southern Ocean cooling linked to tropical variability Nat. Clim. Change 12 461–8
Clem K R and Fogt R L 2015 South Pacific circulation changes and their connection to the tropics and regional Antarctic warming in austral spring, 1979–2012 J. Geophys. Res. Atmos. 120 2773–92
De Lavergne C, Palter J B, Galbraith E D, Bernardello R and Marinov I 2014 Cessation of deep convection in the open Southern Ocean under anthropogenic climate change Nat. Clim. Change 4 278–82
Dee D P et al 2011 The ERA-Interim reanalysis: configuration and performance of the data assimilation system Q. J. R. Meteorol. Soc. 137 553–97
Deser C, Guo R and Lehner F 2017 The relative contributions of tropical Pacific sea surface temperatures and atmospheric internal variability to the recent global warming hiatus Geophys. Res. Lett. 44 7945–54
Ding Q, Steig E J, Battisti D S and Wallace J M 2012 Influence of the tropics on the southern annular mode J. Clim. 25 6330–48
Doddridge E W, Marshall J, Song H, Campin J-M, Kelley M and Nazarenko L 2019 Eddy compensation dampens Southern Ocean sea surface temperature response to westerly wind trends Geophys. Res. Lett. 46 4365–77
Dong S, Gille S T and Sprintall J 2007 An assessment of the Southern Ocean mixed layer heat budget J. Clim. 20 4425–42
Ferreira D, Marshall J, Bitz C M, Solomon S and Plumb A 2015 Antarctic Ocean and sea ice response to ozone depletion: a two-time-scale problem J. Clim. 28 1206–26
Folland C, Renwick J, Salinger M and Mullan A 2002 Relative influences of the interdecadal Pacific oscillation and ENSO on the South Pacific convergence zone Geophys. Res. Lett. 29 21–1–21–4
Fyfe J C, Saenko O A, Zickfeld K, Eby M and Weaver A J 2007 The role of poleward-intensifying winds on Southern Ocean warming J. Clim. 20 5391–400
Gupta A S, Santoso A, Taschetto A S, Ummenhofer C C, Trevena J and England M H 2009 Projected changes to the Southern Hemisphere ocean and sea ice in the IPCC AR4 climate models J. Clim. 22 3047–78
Hall A and Visbeck M 2002 Synchronous variability in the Southern Hemisphere atmosphere, sea ice, and ocean resulting from the annular mode J. Clim. 15 3043–57
Haumann F A, Gruber N and Münnich M 2020 Sea-ice induced Southern Ocean subsurface warming and surface cooling in a warming climate AGU Adv. 1 e2019AV000132
Haumann F A, Gruber N, Münnich M, Frenger I and Kern S 2016 Sea-ice transport driving Southern Ocean salinity and its recent trends Nature 537 89–92
Hirahara S, Ishii M and Fukuda Y 2014 Centennial-scale sea surface temperature analysis and its uncertainty J. Clim. 27 57–75
Huang B, Banzon V F, Freeman E, Lawrimore J, Liu W, Peterson T C, Smith T M, Thorne P W, Woodruff S D and Zhang H-M 2015 Extended reconstructed sea surface temperature version 4 (ERSST. v4). Part I: upgrades and intercomparisons J. Clim. 28 911–30
Huang B, Thorne P W, Banzon V F, Boyer T, Chepurin G, Lawrimore J H, Menne M J, Smith T M, Vose R S and Zhang H-M 2017 Extended reconstructed sea surface temperature, version 5 (ERSSTv5): upgrades, validations, and intercomparisons J. Clim. 30 8179–205
Hurrell J W, Hack J J, Shea D, Caron J M and Rosinski J 2008 A new sea surface temperature and sea ice boundary dataset for the Community Atmosphere Model J. Clim. 21 5145–53
Ibebuchi C C 2021 On the relationship between circulation patterns, the southern annular mode, and rainfall variability in Western Cape Atmosphere 12 753
Ibebuchi C C and Richman M B 2024 Non-linear modes of global sea surface temperature variability and their relationships with global precipitation and temperature Environ. Res. Lett. 19 024001
Jones J M et al 2016 Assessing recent trends in high-latitude Southern Hemisphere surface climate Nat. Clim. Change 6 917–26
Kang S M, Yu Y, Deser C, Zhang X, Kang I-S, Lee S-S, Rodgers K B and Ceppi P 2023 Global impacts of recent Southern Ocean cooling Proc. Natl Acad. Sci. 120 e2300881120
Kobayashi S et al 2015 The JRA-55 reanalysis: general specifications and basic characteristics J. Meteorol. Soc. Japan II 93 5–48
Kosaka Y and Xie S-P 2013 Recent global-warming hiatus tied to equatorial Pacific surface cooling Nature 501 403–7
Kostov Y, Marshall J, Hausmann U, Armour K C, Ferreira D and Holland M M 2017 Fast and slow responses of Southern Ocean sea surface temperature to SAM in coupled climate models Clim. Dyn. 48 1595–609
Latif M, Martin T and Park W 2013 Southern Ocean sector centennial climate variability and recent decadal trends J. Clim. 26 7767–82
Levine A F, Frierson D M and McPhaden M J 2018 AMO forcing of multidecadal Pacific ITCZ variability J. Clim. 31 5749–64
Li X et al 2021 Tropical teleconnection impacts on Antarctic climate changes Nat. Rev. Earth Environ. 2 680–98
Li X, Holland D M, Gerber E P and Yoo C 2014 Impacts of the north and tropical Atlantic Ocean on the Antarctic Peninsula and sea ice Nature 505 538–42
Li X, Holland D M, Gerber E P and Yoo C 2015 Rossby waves mediate impacts of tropical oceans on West Antarctic atmospheric circulation in austral winter J. Clim. 28 8151–64
Li X, Xie S-P, Gille S T and Yoo C 2016 Atlantic-induced pan-tropical climate change over the past three decades Nat. Clim. Change 6 275–9
McGregor S, Timmermann A, Stuecker M F, England M H, Merrifield M, Jin F-F and Chikamoto Y 2014 Recent Walker circulation strengthening and Pacific cooling amplified by Atlantic warming Nat. Clim. Change 4 888–92
Mechoso C R, Losada T, Koseki S, Mohino-Harris E, Keenlyside N, Castaño-Tierno A, Myers T A, Rodriguez-Fonseca B and Toniazzo T 2016 Can reducing the incoming energy flux over the Southern Ocean in a CGCM improve its simulation of tropical climate? Geophys. Res. Lett. 43 11057–063
Mechoso C et al 2014 Ocean–cloud–atmosphere–land interactions in the southeastern Pacific: the VOCALS program Bull. Am. Meteorol. Soc. 95 357–75
Meehl G A, Arblaster J M, Fasullo J T, Hu A and Trenberth K E 2011 Model-based evidence of deep-ocean heat uptake during surface-temperature hiatus periods Nat. Clim. Change 1 360–4
Meehl G A, Hu A, Castruccio F, England M H, Bates S C, Danabasoglu G, McGregor S, Arblaster J M, Xie S-P and Rosenbloom N 2021 Atlantic and Pacific tropics connected by mutually interactive decadal-timescale processes Nat. Geosci. 14 36–42
Meehl G A, Hu A, Santer B D and Xie S-P 2016 Contribution of the Interdecadal Pacific Oscillation to twentieth-century

global surface temperature trends *Nat. Clim. Change* **6** 1005–8
Nuncio M and Yuan X 2015 The influence of the Indian Ocean dipole on Antarctic sea ice *J. Clim.* **28** 2682–90
Pauling A G, Bitz C M, Smith I J and Langhorne P J 2016 The response of the Southern Ocean and Antarctic sea ice to freshwater from ice shelves in an Earth system model *J. Clim.* **29** 1655–72
Power S, Casey T, Folland C, Colman A and Mehta V 1999 Inter-decadal modulation of the impact of ENSO on Australia *Clim. Dyn.* **15** 319–24
Purich A, England M H, Cai W, Sullivan A and Durack P J 2018 Impacts of broad-scale surface freshening of the Southern Ocean in a coupled climate model *J. Clim.* **31** 2613–32
Ruprich-Robert Y, Msadek R, Castruccio F, Yeager S, Delworth T and Danabasoglu G 2017 Assessing the climate impacts of the observed Atlantic multidecadal variability using the GFDL CM2. 1 and NCAR CESM1 global coupled models *J. Clim.* **30** 2785–810
Rye C D, Marshall J, Kelley M, Russell G, Nazarenko L S, Kostov Y, Schmidt G A and Hansen J 2020 Antarctic glacial melt as a driver of recent Southern Ocean climate trends *Geophys. Res. Lett.* **47** e2019GL086892
Sallée J-B, Speer K and Rintoul S 2010 Zonally asymmetric response of the Southern Ocean mixed-layer depth to the southern annular mode *Nat. Geosci.* **3** 273–9
Sen P K 1968 Estimates of the regression coefficient based on Kendall's tau *J. Am. Stat. Assoc.* **63** 1379–89
Sigmond M and Fyfe J 2010 Has the ozone hole contributed to increased Antarctic sea ice extent? *Geophys. Res. Lett.* **37** L18502
Simpkins G R, McGregor S, Taschetto A S, Ciasto L M and England M H 2014 Tropical connections to climatic change in the extratropical Southern Hemisphere: the role of Atlantic SST trends *J. Clim.* **27** 4923–36
Simpkins G R, Peings Y and Magnusdottir G 2016 Pacific influences on tropical Atlantic teleconnections to the Southern Hemisphere high latitudes *J. Clim.* **29** 6425–44
Slivinski L C *et al* 2019 Towards a more reliable historical reanalysis: improvements for version 3 of the twentieth century reanalysis system *Q. J. R. Meteorol. Soc.* **145** 2876–908
Smith T M, Reynolds R W, Peterson T C and Lawrimore J 2008 Improvements to NOAA's historical merged land–ocean surface temperature analysis (1880–2006) *J. Clim.* **21** 2283–96
Stevens B, Sherwood S C, Bony S and Webb M J 2016 Prospects for narrowing bounds on Earth's equilibrium climate sensitivity *Earth's Future* **4** 512–22
Thompson D W and Wallace J M 2000 Annular modes in the extratropical circulation. Part I: month-to-month variability *J. Clim.* **13** 1000–16
Xu X, Liu J and Huang G 2022 Understanding sea surface temperature cooling in the central-east Pacific sector of the Southern Ocean during 1982–2020 *Geophys. Res. Lett.* **49** e2021GL097579
Yao S L, Zhou W, Jin F F and Zheng F 2021 North Atlantic as a trigger for Pacific-wide decadal climate change *Geophys. Res. Lett.* **48** e2021GL094719
Yao S-L, Luo J-J, Chu P-S and Zheng F 2023 Decadal variations of Pacific Walker circulation tied to tropical Atlantic–Pacific trans-basin SST gradients *Environ. Res. Lett.* **18** 064016
Yao S-L, Luo J-J, Huang G and Wang P 2017 Distinct global warming rates tied to multiple ocean surface temperature changes *Nat. Clim. Change* **7** 486–91
Yuan X, Kaplan M R and Cane M A 2018 The interconnected global climate system—a review of tropical–polar teleconnections *J. Clim.* **31** 5765–92
Zelinka M D *et al* 2020 Causes of higher climate sensitivity in CMIP6 models *Geophys. Res. Lett.* **47** e2019GL085782
Zhang L, Delworth T L, Cooke W and Yang X 2019 Natural variability of Southern Ocean convection as a driver of observed climate trends *Nat. Clim. Change* **9** 59–65
Zhang X, Deser C and Sun L 2021 Is there a tropical response to recent observed Southern Ocean cooling? *Geophys. Res. Lett.* **48** e2020GL091235